Artificial Enzymes from Hafnium Diboride Nanosheets Dispersed in Biocompatible

Block Copolymers

by

Mahmoud Matar Abed

A Thesis Presented in Partial Fulfillment
of the Requirements for the Degree
Master of Science

Approved November 2019 by the
Graduate Supervisory Committee:

Qing Hua Wang, Co-Chair
Alexander Green, Co-Chair
Yang Jiao

ARIZONA STATE UNIVERSITY

December 2019

ABSTRACT

Nanomaterials that exhibit enzyme-like catalytic activity or nanozymes have many advantages compared to biological enzymes such as low cost of production and high stability. There is a substantial interest in studying two-dimensional materials due to their exceptional properties. Hafnium diboride is a type of two-dimensional material and belongs to the metal diborides family made of hexagonal layers of boron atoms separated by metal layers. In this work, the peroxidase-like activity of hafnium diboride nanoflakes dispersed in the block copolymer F77 was discovered for the first time. The kinetics, mechanisms and catalytic performance towards the oxidation of the chromogenic substrate 3,3,5,5-tetramethylbenzidine (TMB) in the presence of hydrogen peroxide are presented in this work. Kinetic parameters were determined by steady-state kinetics and a comparison with other nanozymes is given. Results show that the HfB_2/F77 nanozyme possesses a unique combination of unusual high affinity towards hydrogen peroxide and high activity per cost. These findings are important for applications that involve reactions with hydrogen peroxide.

DEDICATION

I would like to dedicate this thesis to my family that have supported me throughout my whole life and career.

ACKNOWLEDGMENTS

I wish to thank my advisors Dr. Qing Hua Wang and Dr. Alexander Green for the opportunity to work in their laboratory and provide me with the experience to grow as a researcher. I would like to thank Dr. Yang Jiao for agreeing to be in my committee. Thanks to all the members of Dr. Wang and Dr. Green groups for their support throughout graduate school.

TABLE OF CONTENTS

iv

LIST OF TABLES

LIST OF FIGURES

Chapter 1

Introduction and Motivation

Enzymes are biological catalysts found in nature and play the crucial role of accelerating reaction rates and include important functions in living organisms such as DNA production and cell communication. Many applications like water purification, pharmaceutical and food industries also use natural enzymes for specific reactions.[1–3] However, enzymes have the disadvantage of high production cost and low stability.[4,5] Researchers have developed artificial enzymes to tackle the disadvantages related to natural enzymes.[6] Nanozymes are nanomaterials with enzyme-like activities, or enzyme mimics. The first appearance of the term nanozyme was for the discovery of peroxidase mimicking activity in magnetite nanoparticles.[7]
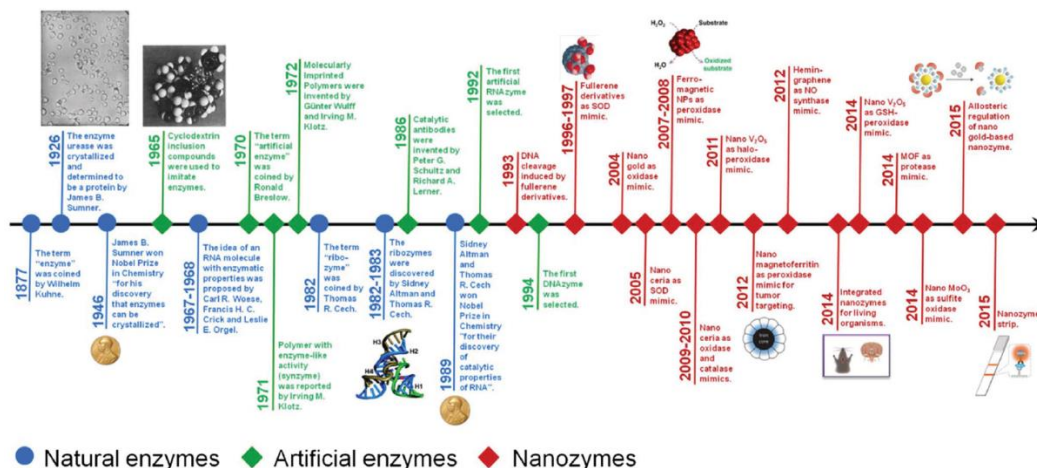
Schematic 1: Development of artificial enzymes and nanozymes through the years.

Adapted from Wang *et. al.*[6]

This study is focused on understanding the peroxidase-like activity of a new type of nanozyme made of hafnium diboride (HfB$_2$) nanosheets dispersed in the block copolymer F77. The details of the kinetics, mechanisms and catalytic performance are presented in this work. First, we show materials characterization of the HfB2 nanosheets dispersed in F77 including morphology, thickness and composition are shown. Second, the catalytic activity of the nanozyme towards the oxidation of 3,3,5,5-tetramethylbenzidine (TMB) in the presence and reduction of hydrogen peroxide is studied in detail. Steady-state kinetics were employed to determine relevant kinetic parameters and reveal the reaction mechanism of this catalytic reaction. Finally, the HfB$_2$/F77 nanozyme is compared against other nanozymes in terms of its catalytic performance and cost effectiveness.

Chapter 2

Background

Nanozymes are classified based on the natural enzymatic reaction that they mimic. Thus, they are generally divided into two different families: oxidoreductases and hydrolases.[8] The oxidoreductase mimics include oxidase, peroxidase, catalase, superoxide dismutase and nitrate reductase mimics. The hydrolase mimics include mimics of nuclease, esterase, phosphatase, protease and silicatein.[8] There is a wide spectrum of applications in which nanozymes have been used, ranging from biosensing, cancer therapy, to antibacterial and more (**Schematic 2**). There is also a wide assortment of morphologies that have been reported for nanozymes including nanoparticles, nanoflakes, nanocubes, quantum dots, and nanotubes. Peroxidase is a natural enzyme that catalyzes the reduction of hydrogen peroxide and oxidation of a specific substrate like TMB. Natural peroxidases such as horseradish peroxidase (HRP) are employed in applications that range from wastewater treatment to enzyme immunoassays. [9,10] Horseradish peroxidase is a heme peroxidase produced from the roots of horseradish plants. Advantages of using HRP include high turnover number and small size but it has limitations in production cost and stability.[11] A colorimetric assay can be done to determine peroxidase activity testing different peroxidase substrates.[12]

Two-dimensional materials are composed of atomic layers stacked together. Most 2D materials have van der Waals (vdW) attractive forces between atomic layers like transition metal dichalcogenides (TMDCs).[13] On the other hand, some layered nanomaterials are known as non-vdW 2D materials because different kind of atomic interaction occurs between layers.[14] Layers of 2D materials can be exfoliated by solution

phase processing by ultrasonication in dispersants such as organic solvents and aqueous solutions of surfactants.[15] Among these, Pluronic F77 is an amphiphilic, water soluble, and biocompatible block-copolymer used in medical applications,[16] and which can disperse nanomaterials.[17] Pluronic F77 is a triblock copolymer with alternating hydrophilic poly(ethylene oxide) (PEO) and hydrophobic poly(propylene oxide) (PPO) blocks (**Figure 1**).
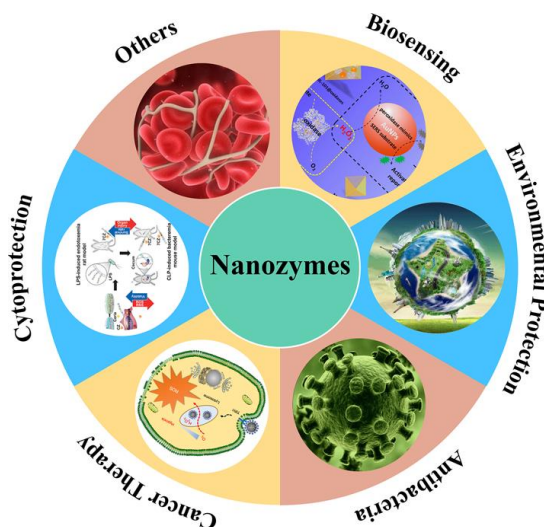
Schematic 2: Applications of nanozymes. Adapted from Huang *et. al.*[8]

Metal diborides (MB$_2$) are ultra-high temperature ceramics[18] that exhibit exceptional thermal, chemical, and mechanical stability and possess a common layered crystal structure consisting of hexagonal layers of boron atoms separated by metal layers (**Figure 1**). There is a mixed ionic-covalent type of bonding between boron and metal layers.[19] Different MB$_2$ materials like ZrB$_2$, CrB$_2$ and TaB$_2$ were tried for liquid phase exfoliation with F77 and screened for peroxidase activity from which HfB$_2$ was the most

promising. In this work, hafnium diboride a type MB_2 will be dispersed in F77 through liquid phase exfoliation to study the peroxidase-like activity of HfB_2/F77.
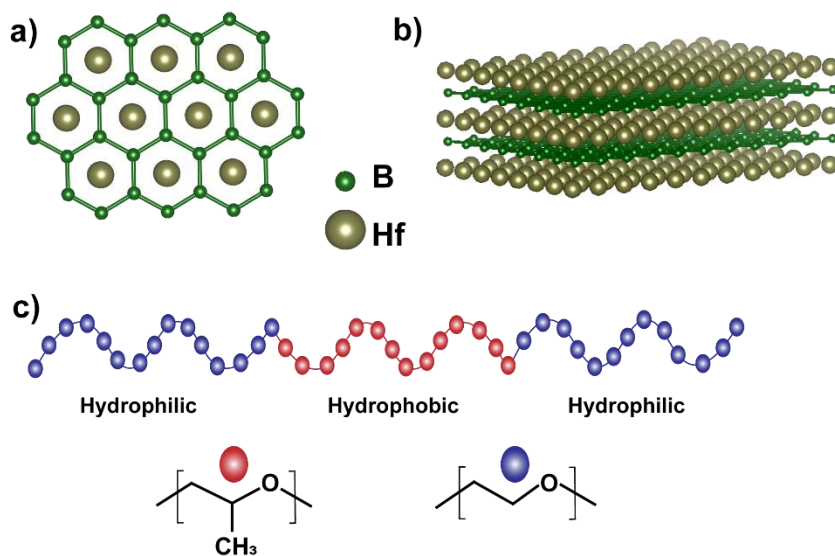

Figure 1: Structure of HfB₂ and F77. Schematic of the a) top view and b) lateral view of HfB_2 crystal structure. c) Structure of the block copolymer F77.

Chapter 3

Experimental Methods

3.1 Materials

Hafnium diboride powder was obtained from Smart Elements. Pluronic F77 Micropastille was obtained from BASF. 3,3,5,5-tetramethylbenzidine (TMB), o-phenylenediamine (OPD), 2,2'-azino-bis(3-ethylbenzothiazoline-6-sulphonic acid) (ABTS), di-azo-aminobenzene (DAB), 30 wt. % hydrogen peroxide solution and sodium acetate buffer solution were purchased from Sigma Aldrich.

3.2 HfB$_2$ Dispersion

HfB$_2$ nanoflakes were dispersed in Pluronic F77 by liquid-phase exfoliation employing a Branson Digital Sonifier®. A typical procedure consisted of adding 200 mg of HfB$_2$ powder in 5mL of aqueous F77 solution, followed by ultrasonication with a 13-mm tip at 26% amplitude and specific time. Then the bulk material was removed by centrifugation for 5 minutes at 5000 RCF. The mass concentration of HfB$_2$ was determined from the molar extinction coefficient obtained by inductively coupled plasma mass spectrometry (ICP-MS) and measuring absorbance at 600 nm in a Synergy H1 Hybrid Multi-Mode Reader (BioTek).

3.3 Nanomaterial Characterization

The exfoliated nanoflakes were characterized by atomic force microscopy (AFM), transmission electron microscopy (TEM), high-resolution transmission electron microscopy (HR-TEM) and energy dispersive spectroscopy (EDS).

Samples for AFM imaging were prepared by spin-coating 20 μL of dispersion on a silicon substrate at 2500 RPM for one minute. This step was repeated three times. Then the sample was annealed under argon gas for three hours at 300ºC. The images were obtained by a Bruker Multimode V AFM and processed by Gwyddion software. The thickness distribution on Figure 4b was made by measuring the thickness of 200 nanoflakes from AFM images employing Gwyddion.

TEM images were generated on Philips CM-12 TEM operated at 80kV and acquired with a Gatan model 791 CCD camera using holey carbon grids. TEM samples were prepared by drop-casting a small volume of dilute dispersion on the grid, which was dried under ambient conditions. HRTEM samples were prepared by drop-casting HfB_2/F77 dispersions onto lacey carbon grids (Cu-400LC, Pacific Grid Tech). Imaging and EDS analysis were performed using a FEI Titan operating at an accelerating voltage of 300 kV. TEM imaging was done by Sanchari Saha. HR-TEM and EDS data was obtained by Matthew Gilliam. For the size distribution of nanoflakes (**Figure 6d**), ImageJ was used on TEM images to calculate the area of 200 nanoflakes (**Figure 6c**).

3.4 Catalytic Activity

3.4.1 Screening for Peroxidase-like Activity

In the colorimetric assay to determine peroxidase-like activity, the typical peroxidase colorimetric substrates 3,3,5,5-tetramethylbenzidine (TMB), o-phenylenediamine (OPD), 2,2'-azino-bis(3-ethylbenzothiazoline-6-sulphonic acid) (ABTS) and di-azo-aminobenzene (DAB) were used. The reactions were carried out in 1.5

mL microtubes. The reaction solutions were composed of 0.2 M acetate buffer, 1M H_2O_2, 4 µg/mL HfB_2 and 2 mM of each respective peroxidase substrate.

3.4.2 Catalytic Activity Characterization

The peroxidase-like activity of HfB_2 nanozyme was studied with the colorimetric TMB substrate on 96-well plates and the absorbance of the oxidized TMB was measured with the Synergy H1 multi-plate reader at a wavelength of 652 nm.

For the nanozyme catalytic characterization in terms of ultrasonication time, pH, temperature, H_2O_2 concentration and TMB concentration, just one parameter was varied while the rest of the conditions were fixed, and absorbance was measured after 10 minutes of reaction. The highest absorbance was set as 100% relative activity in all the assays. The final working concentration of nanozyme was 4 µg/mL HfB_2 in all experiments.

For the optimal pH determination, the experiment was carried out at 37ºC, 0.2 M sodium acetate buffer, 1 M H_2O_2, 2 mM TMB, and varying pH from pH 2 to pH 12. The relative activity at different TMB concentrations was studied at 37ºC with reaction mixtures of 0.2 M pH 4 sodium acetate buffer, 10 mM H_2O_2, and varying TMB concentrations from 1 mM to 9 mM. The catalytic activity at different H_2O_2 concentrations was studied at 37ºC with reaction mixtures of 0.2 M pH4 sodium acetate buffer, 7 mM TMB, and varying H_2O_2 concentrations from 5 mM to 300 mM. The optimal temperature was determined by studying different temperatures (10-100ºC) and the concentrations in the reaction were 0.2 M pH 4 sodium acetate buffer, 7 mM TMB, and 10mM H_2O_2.

3.4.3 Steady State Kinetics

The kinetic experiments were carried out by measuring the absorbance change with time. The initial rate velocity was determined by linear regression analysis of the change in absorbance and time on the early stage of the reaction. Then the initial velocity of the reaction and the substrate concentrations were fitted to the Michalis-Menten equation (**Eq. 1**). All the kinetic experiments were done with a fixed concentration of 4 µg/mL HfB_2 nanozyme, 0.2 M acetate buffer pH 4 and 37ºC. The kinetic parameters of TMB were determined by fixing the concentration of H_2O_2 to 10 mM. On the other hand, for H_2O_2 kinetic parameters, the concentration of TMB was fixed to 7 mM.

3.4.4 Reaction Mechanism

The reaction mechanism was studied with the double reciprocal plot of the initial rate velocity and substrate concentration. These experiments were made with a fixed concentration of 4 µg/mL HfB_2 nanozyme, 0.2 M acetate buffer pH 4 and 37ºC. For the double reciprocal plot of TMB; three different experiments were done having three different concentrations of H_2O_2 (1, 2 and 5 mM) and varying the concentration of TMB for each experiment. The opposite was done for the double reciprocal plot of H_2O_2 and the three different concentrations of TMB were 1 mM, 3 mM, and 5 mM.

Results: Preparation and Characterization of HfB$_2$/F77 Nanozyme

4.1 Dispersion of HfB$_2$ in F77

Two-dimensional nanomaterials can be dispersed in aqueous solutions with the aid of dispersing agents and ultrasound waves. Layers get separated because of cavities produced from ultrasound waves in the sonication process.[20] Subsequently, adsorption of the dispersing agent on the nanoflakes leads to their stabilization by electrostatic repulsion.[21] Hafnium diboride nanozyme dispersed in F77 (**Figure 2**) was prepared by probe ultrasonication of 200 mg of powder in 5 mL of aqueous F77 with 26% power for 5 hours. The unexfoliated material was removed by centrifugation.
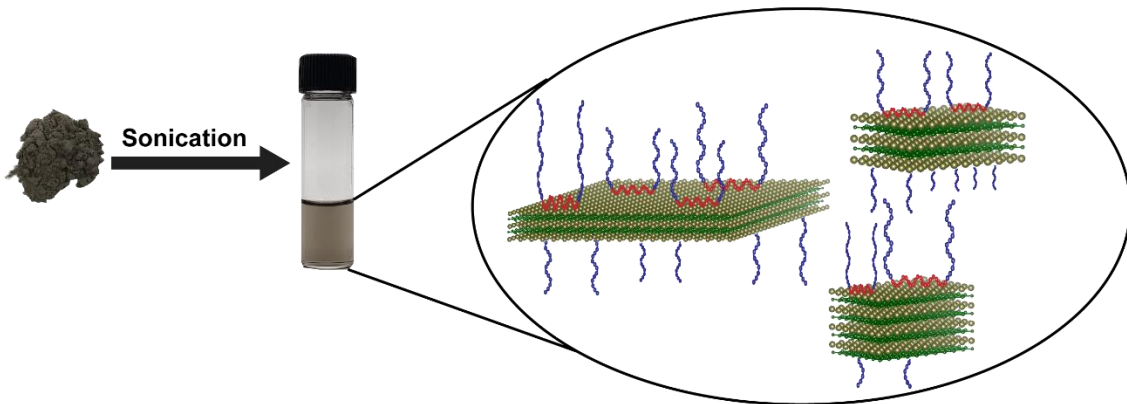

Figure 2: Schematic of the liquid-phase exfoliation of HfB$_2$ by F77.

4.1.1 Optimization of exfoliation

To optimize the concentration of HfB_2 in the liquid-phase exfoliation, different percentages of F77 were used. The same procedure described above was followed, but different mass percentages of F77 were used: 2%, 3%, and 4%. From visual inspection of the dispersions after sonication and removal of bulk undispersed material by centrifugation (**Figure 3**), the exfoliation yielding seems to be optimized with 3% F77. A higher concentration of F77 (4%) makes the nanoflakes exfoliation less effective because of surface tension reduction caused by the concentration of dispersing agent.[22] Lower F77 concentration (2%) is not as effective as 3% F77 because that concentration of dispersing agent is not enough to keep the separated layers of HfB_2 stabilized in solution.
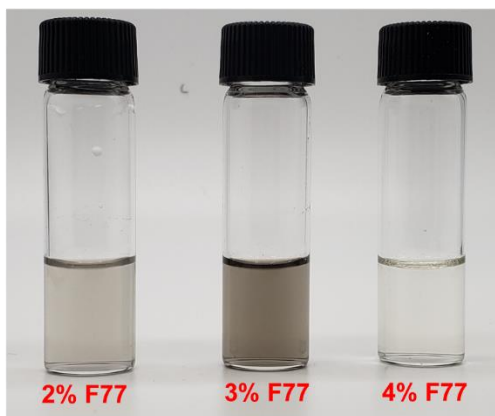

Figure 3: Optimization of HfB₂ concentration in F77 dispersions. Dispersions after probe ultrasonication for 5 h followed by centrifugation.

4.2 Characterization of HfB₂/F77 Dispersion

Hafnium diboride nanoflakes exfoliated by F77 were characterized by techniques such as atomic force microscopy (AFM), transmission electron microscopy (TEM), high-resolution transmission electron microscopy (HR-TEM) and energy dispersive spectroscopy (EDS).

4.2.1 Atomic Force Microscopy

The topographic morphology of the nanozyme was studied by AFM. Dispersed nanoflakes were spin-coated in silicon wafers followed by annealing treatment to get rid of F77 or any contamination. The nanoflakes exhibit different thicknesses and areas (**Figures 4 and 5**). Additionally, from the AFM images we can see nanoflakes stacked together. A histogram of the flake thickness distribution was made from the AFM images using 200 nanoflakes (**Figure 6a**). The average thickness was 13.9 nm(**Figure 6b**).
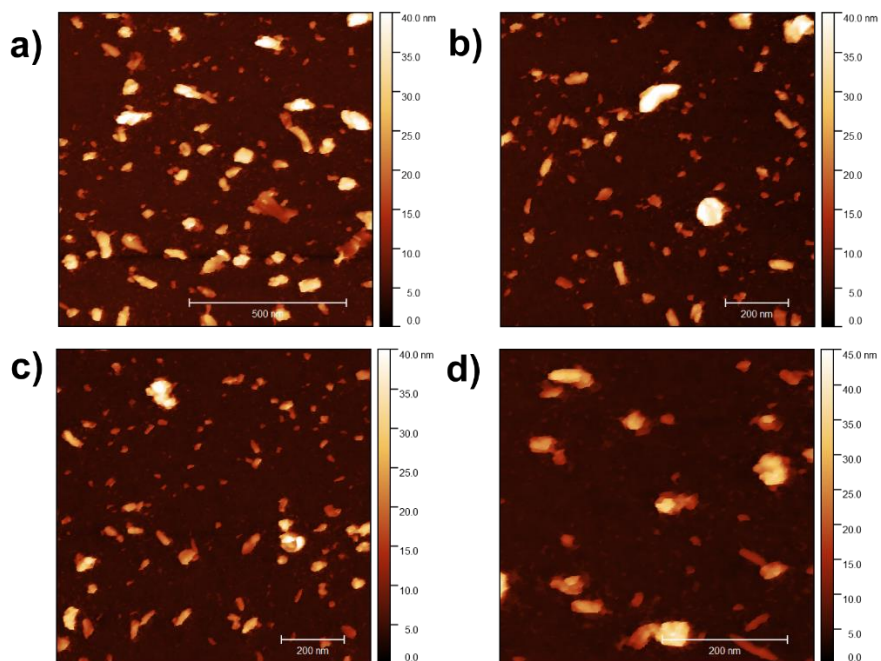
Figure 4: AFM Images of HfB$_2$ liquid exfoliation by F77.

4.2.2 Transmission Electron Microscopy

TEM was employed to image the nanozyme dispersion. Different sizes of nanoflakes are produced and stacking of nanoflakes is noticeable like in the AFM images. Size distribution of nanoflakes was made with 200 nanoflakes and the average area was 967 nm^2 (**Figure 6d**).
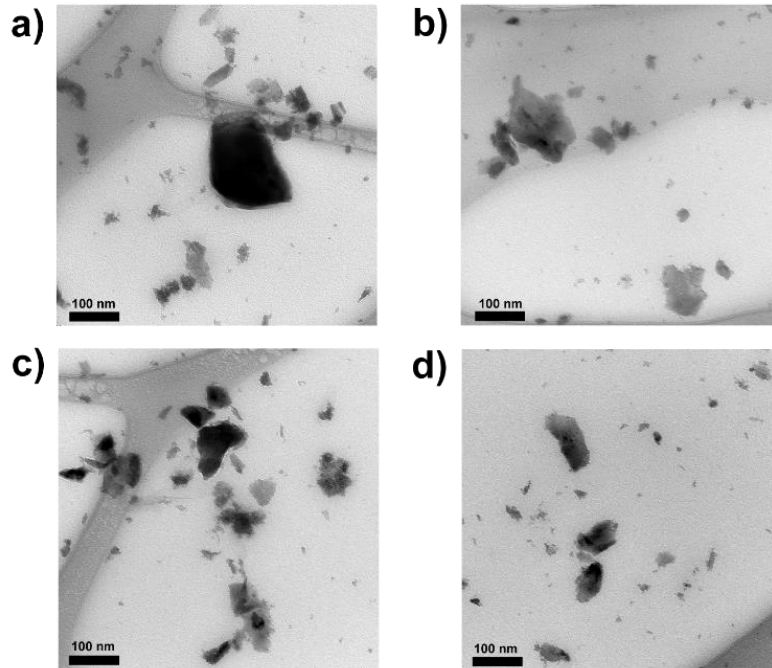
Figure 5: TEM Images of HfB₂ liquid exfoliation by F77.

4.2.3 HR-TEM and EDS Analysis

HR-TEM images and EDS spectrum were obtained for the HfB$_2$ nanoflakes dispersed in F77 (**Figure 7**). Despite the difficulty of seeing the atomic pattern of the nanoflakes HR-TEM caused by the presence of F77 on the flakes, some hexagonal atomic order can be seen from the HR-TEM image (**Figure 7b**). The presence of hafnium in the flakes was confirmed from the EDS spectrum. (**Figure 7c**) Furthermore, the hafnium characteristic peak around 2 keV disappeared when the measurement was taken off the flake. The copper peak at 8 keV corresponds to the grid and there is a small Ti peak caused by some impurities. C and O peaks are also found, and they might correspond to F77 sitting on the surface, or some minor oxidation of the HfB$_2$ flakes during processing.
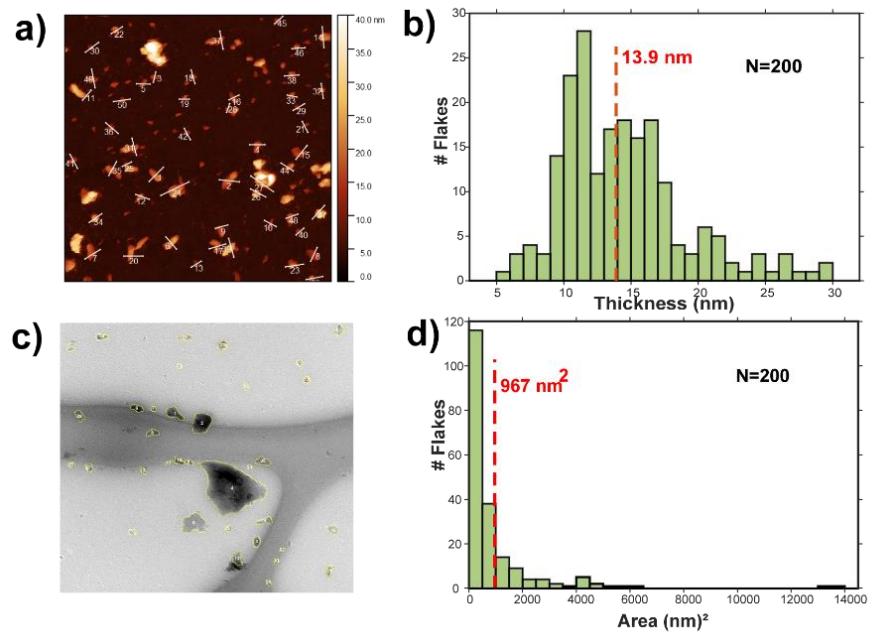
Figure 6: Thickness and size distribution of nanozyme. a) Example of an AFM image used for thickness measurements. b) Thickness distribution of 200 nanoflakes with 13.9 nm the average thickness. c) Example of a TEM image used for measuring the areas of the flakes. d) Size distribution of 200 nanoflakes with 967 nm^2 the average area.
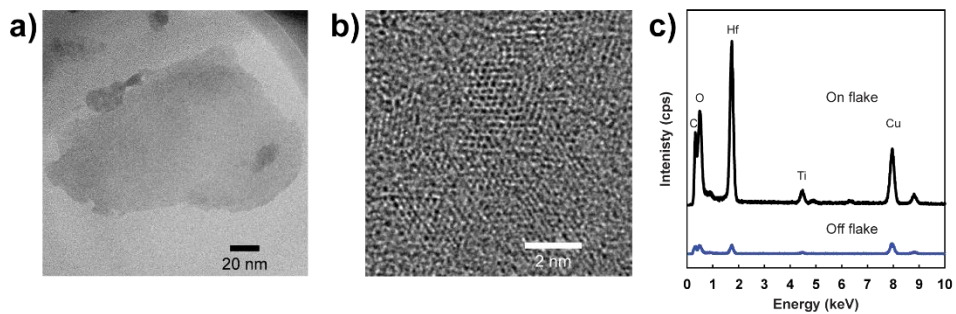
Figure 7: HR-TEM and EDS data. a) TEM image of a nanoflake and corresponding b) HR-TEM image c) EDS spectrum on and off the flake.

Chapter 5

Results: Catalytic Activity of HfB$_2$/F77

A common chromogenic peroxidase substrate 3,3,5,5-tetramethylbenzidine (TMB) is used to study enzyme mimics with peroxidase-like activity due to its high sensitivity and highest molar extinction coefficient among the known colorimetric substrates. TMB can be oxidized by peroxidase in the presence of H$_2$O$_2$ displaying a blue color with maximum absorbance at 652 nm. The oxidation mechanism for this reaction involves two steps of single electron oxidation.[23] The peroxidase-like activity of HfB$_2$/F77 is described in (**Figure 9a)** where TMB is oxidized by the nanozyme dispersion in the presence of H$_2$O$_2$. This colorimetric reaction can then be analyzed by measuring the absorbance at 652 nm.

5.1 Intrinsic peroxidase-like activity of nanozyme

To confirm the ability of HfB$_2$/F77 nanozyme to mimic the catalytic reaction of natural peroxidase, a screening for peroxidase activity was performed (**Figure 8**). Four commonly used substrates were utilized for this inspection; 3,3,5,5-tetramethylbenzidine (TMB), o-phenylenediamine (OPD), 2,2'-azino-bis(3-ethylbenzothiazoline-6-sulphonic acid) (ABTS) and di-azo-aminobenzene (DAB). After 10 minutes of reaction, typical color changes for the oxidation of these substrates were clearly visible. TMB, OPD, ABTS, and DAB upon oxidation turn blue, yellow, green, and brown, respectively.
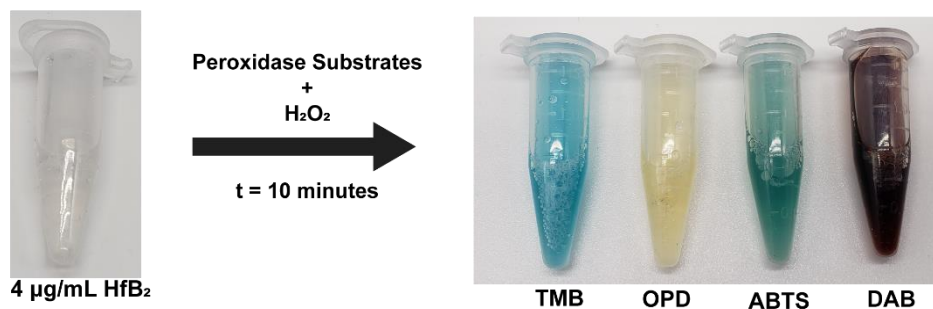
Figure 8: Screening for peroxidase-like activity of HfB$_2$/F77. Images taken after 10 minutes of reaction with 4 μg/mL HfB$_2$/F77, 7 mM of substrate (each substrate is listed under the respective vial), 10 mM H$_2$O$_2$ in 0.2 M acetate buffer at pH 4.

To demonstrate the importance of dispersing the nanoflakes for the catalytic reaction, a comparison between exfoliated HfB$_2$ nanoflakes and undispersed powder HfB$_2$ was done (**Figure 9b**). The powder sample had a concentration about 5000 times higher than the exfoliated HfB$_2$ sample. Despite this, the exfoliated sample showed a more intense blue color change corresponding to higher yielding of oxidized TMB. When the nanoflakes are exfoliated, more surface area and edges are exposed, all contributing to the improved catalytic activity.

From the peroxidase-like activity screening and comparison with unexfoliated HfB$_2$ we demonstrated the existence of intrinsic peroxidase-like activity in HfB$_2$ nanoflakes.
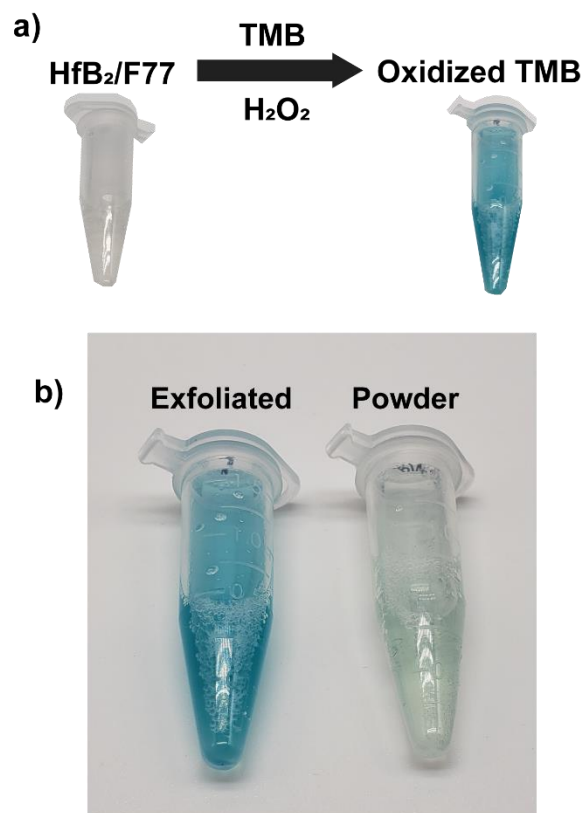
Figure 9: Peroxidase-like catalytic activity description. a) Description of the catalytic oxidation of TMB by the nanozyme in presence of H_2O_2. b) Comparison of exfoliated HfB_2/F77 and HfB_2 powder. TMB oxidation reactions after 10 minutes of exfoliated nanoflakes vs bulk powder.

5.2 Characterization of the catalytic reaction

In order to obtain the optimal performance of HfB_2/F77 nanozyme, we systematically varied the experimental conditions of preparing the nanozyme and performing the enzymatic reaction. First, the catalytic activity of dispersions prepared using the different probe ultrasonication durations was studied (**Figure 10**). Then, the other

parameters examined were pH, temperature, TMB concentration and H_2O_2 concentration (**Figure 11**).

In **Figure 10** the absorbance change of the catalytic reaction with time was measured for HfB_2 nanoflake dispersions prepared with varying durations of ultrasonication. The highest activity was achieved with 5 hours sonication compared with 2 h and 10 h sonication. Hence, the optimal sonication time for HfB_2/F77 production was determined to be 5 h and was chosen for all subsequent experiments. We speculate that at 2 h, not enough nanoflakes have been generated, so the overall activity is lower, and that at 10 h there may be too much defect generation that decreases the activity.
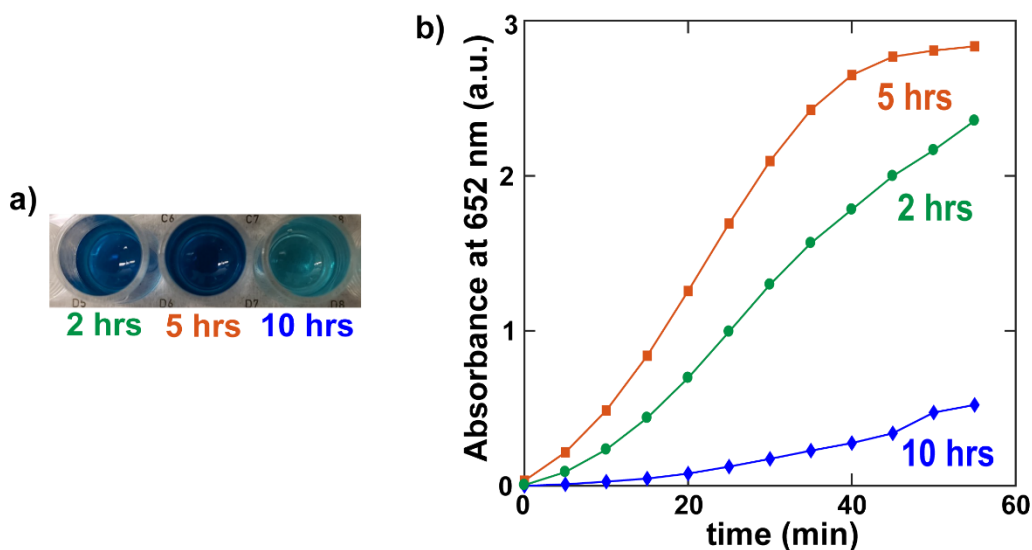

Figure 10: Activity of nanozyme prepared with different sonication times. The three samples have the same concentration of HfB_2.

The roles of other factors in the catalytic reaction were examined systematically as shown in **Figure 11**. The catalytic activity as a function of concentration of TMB is shown

in **Figure 11a**. The highest values of catalytic activity occur at a TMB concentration between 4 to 7 mM, with more than 90% of relative activity achievable in this range. The optimal H_2O_2 concentration for the nanozyme activity was found to be at 10 mM, although the nanozyme can achieve 80% or more of its maximum activity in the entire range of H_2O_2 concentrations that was tested (5 mM to 300 mM). The highest activity was attained at a solution pH of 4. Like the natural horseradish peroxidase (HRP) and other peroxidase-mimics[24–26], the HfB_2/F77 nanozyme achieves high catalytic activity in acidic pH. The optimal temperature for the peroxidase-like activity was found to be 35ºC, and more than 60% of relative activity was obtained in the range from 30ºC to 45ºC. Thus, after completing this series of systematic studies we found that the optimal conditions for the peroxidase-like activity of HfB_2/F77 nanozyme were to be TMB concentration of 7 mM, H_2O_2 concentration of 10 mM, pH of 4 and temperature of 35ºC.
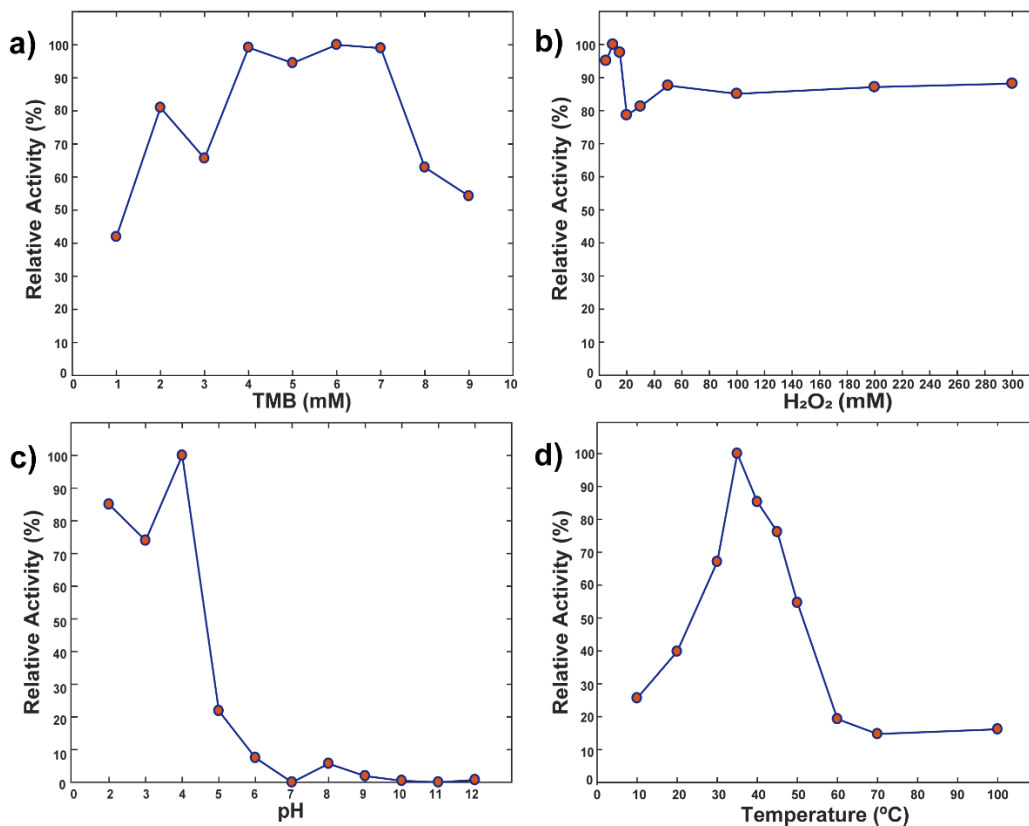
Figure 11: Optimal parameters for the peroxidase-like activity. Relative catalytic activity as a function of different conditions: a) TMB concentration, b) H_2O_2 concentration, c) pH and d) temperature. The highest activity was set as 100% in each plot.

5.3 Steady-State Kinetics and Reaction Mechanism

Understanding the kinetics of a catalytic reaction is fundamental for all enzymes and enzyme-mimics. Researchers have followed the approach of steady-state kinetics and the theory developed by Leonor Michaelis and Maud Leonora Menten. Michaelis and Menten are recognized as the founders of modern enzymology, they developed the *Michaelis-Menten equation* and it is the fundamental equation of enzyme kinetics. The

modern Michaelis-Menten equation employed is derived based on the steady-state assumption:

$$V = \frac{V_{max} \times [S]}{(K_M + [S])}$$

where V is the initial reaction rate, V_{max} is the maximum rate, K_M is the Michaelis constant and S is the substrate concentration. V_{max} is the maximum rate reached in the reaction and corresponds to the velocity where the substrate is saturated. K_M is a catalytic constant that describes the affinity of the substrate to the catalyst and it is the concentration at half the maximum velocity V_{max}. Their approach is based on measuring the initial rates of the catalytic reaction at different substrate concentrations to avoid factors that affect catalysis like product inhibition or reverse reactions.

Two relevant kinetic parameters are determined from the Michaelis-Menten equation; V_{max} and K_M. Insights about the reaction mechanism can be obtained from these parameters. The binding affinity of a specific substrate to the catalyst is measured by the intrinsic parameter K_M.[27] High values of K_M correspond to weak binding between catalyst and substrate. On the other hand, lower K_M is an indication of large binding affinity. Further details of the catalytic reaction mechanism can be gathered with the double reciprocal plots of the Michaelis-Menten equation:

$$\frac{1}{V} = \left(\frac{K_M}{V_{max}}\right)\left(\frac{1}{[S]}\right) + \frac{1}{V_{max}}$$

The corresponding plots are known as the Lineweaver-Burk plots. A well-known mechanism for HRP is called the Ping-Pong mechanism which can be confirmed by parallel lines of double-reciprocal plots.[28] This specific double-reciprocal plot feature is a typical indicator that one substrate will bind to the catalyst first and just after the release of

the product, the second substrate binds and react. The catalytic rate constant (k_{cat}) can be determined by the following equation:

$$k_{cat} = \frac{V_{max}}{[E]}$$

where [E] is the molar concentration of catalyst. The rate constant, also known as the turnover number, measures the amount of substrate converted to product by unit time. The turnover number represents the ability of forming product after the binding between substrate and catalyst.

Nanomaterials that behave as enzyme mimics follow the Michaelis-Menten fitting just as natural enzymes. Steady-state kinetics were employed to gain insights into the reaction mechanism of HfB_2/F77 nanozyme in the oxidation of TMB and reduction of H_2O_2. We determined the catalytic constants by measuring the initial reaction rates at different substrate concentrations and fitting the data to the Michaelis-Menten equation.

The kinetics assay of HfB_2/F77 was done for TMB and H_2O_2 as substrates (**Figure 12**). Both substrates followed the Michaelis-Menten fitting curve. A maximum velocity of 1.98 x 10^{-7} M/s was determined for TMB and 3.20 x 10^{-8} M/s for H_2O_2. The Michaelis constants obtained were 2.71 mM for TMB and 0.183 for H_2O_2. Lower values of K_M indicate higher affinity between the substrate and the nanozyme. HfB_2/F77 seems to have higher binding affinity for H_2O_2 than for TMB based on the Michaelis constants of TMB and H_2O_2. Furthermore, the nanozyme have lower K_M for H_2O_2 than HRP (**Table 1**). HfB_2/F77 nanozyme require higher concentration of TMB to reach the maximal catalytic activity at V_{max} compared to HRP. The higher affinity to H_2O_2 explains the reason behind the lower H_2O_2 concentration needed to reach maximal catalytic activity.
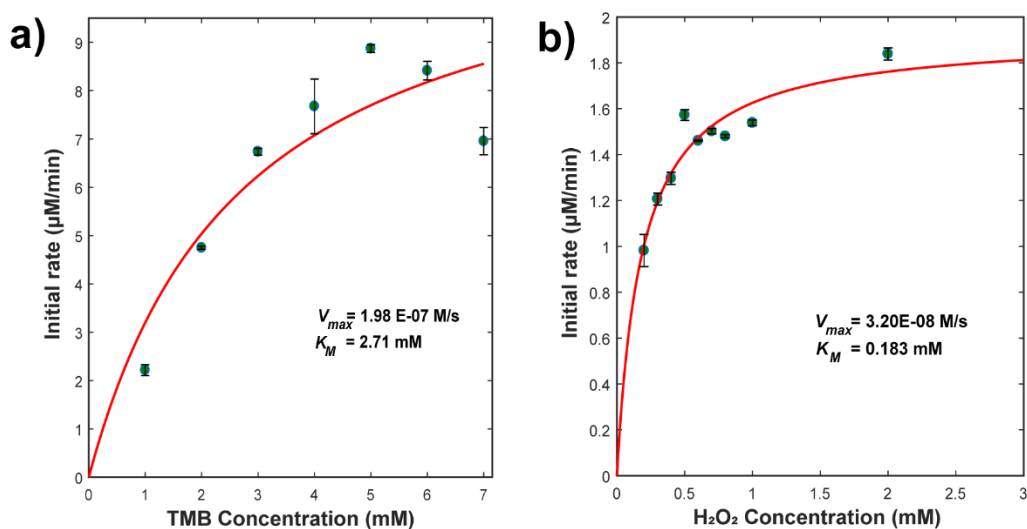
Figure 12: Steady-state kinetic experiments. a) and c) are Michalis-Menten plots for TMB and H_2O_2, respectively. The error bars represent the standard error of three repeated measurements.

The calculated (k_{cat}) for HfB_2 nanozyme was 0.010 s^{-1} and 0.0016 s^{-1} for TMB and H_2O_2, respectively. The turnover number calculated (k_{cat}) is the measure of substrate molecules produced from reacting with HfB_2 molecules per second as the maximum velocity (V_{max}) is reached.

Catalyst	Substrate	K_M (mM)	V_{max} (M/s)
HfB$_2$/F77	TMB	2.710	1.98×10^{-7}
	H$_2$O$_2$	0.185	3.27×10^{-8}
HRP[24]	TMB	0.434	1.00×10^{-7}
	H$_2$O$_2$	3.7	8.78×10^{-8}

Table 1: Kinetic parameters of HfB$_2$/F77 and HRP.

Details about the reaction mechanism involving TMB and H$_2$O$_2$ with the nanozyme can be understood by comparing results with the natural peroxidase HRP. Specifically, with Lineweaver-Burk (double-reciprocal) plots of both substrates. The double reciprocal graphs were made by fixing concentrations of one substrate while the other substrate's concentration varies (**Figure 13**). The lines are parallel confirming that the reaction between the substrates and HfB$_2$/F77 follows a Ping-Pong mechanism which reveals that one substrate will first get attached to the nanozyme and after the product is formed, the second substrate will interact with the nanozyme.[28] This mechanism is common among other nanozymes with intrinsic peroxidase-like activity.[29–31]

The kinetic parameters of the reaction between the nanozyme, TMB and H$_2$O$_2$ substrates were determined. The results showed that HfB$_2$/F77 nanozyme have higher affinity towards H$_2$O$_2$ when compared to the affinity towards TMB. Furthermore, the higher value of K_M corresponding to TMB is an indication that high concentrations of the substrate are necessary in order to achieve maximal activity. This result implies that HfB$_2$/F77 have the capability to prevail against hindrance caused by high TMB concentrations making the nanozyme capable to function in extreme conditions.[26] The

catalytic reaction follows a Ping-Pong mechanism involving both substrates like in the case of HRP.
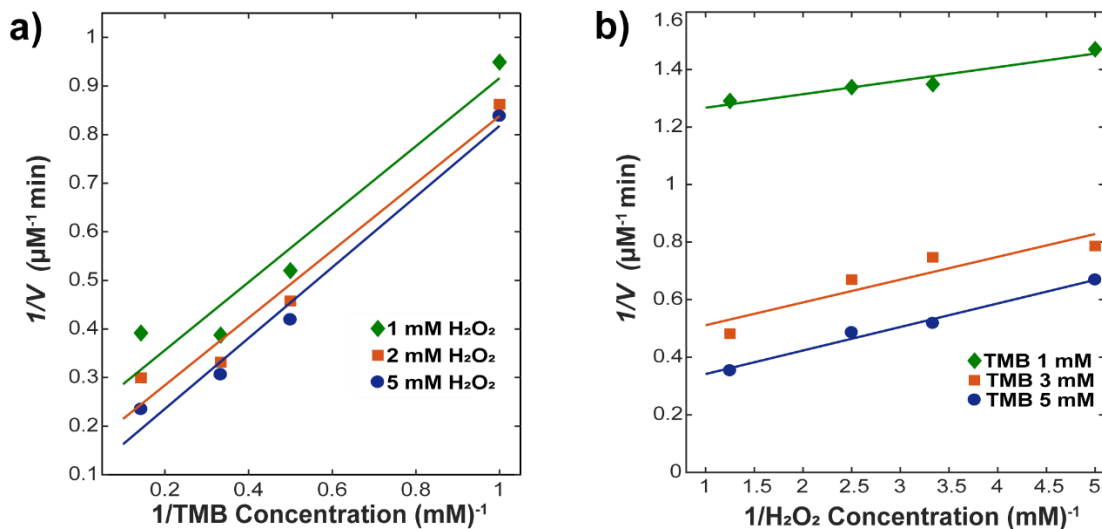
Figure 13: Ping-Pong Mechanism. Double-reciprocal plots (Lineweaver-Burk) for a) TMB and b) H_2O_2. The final working concentration of the nanozyme was 4 µg/mL and all experiments were made at pH 4 and 35ºC.

5.4 Comparison of Catalytic Performance

Applications of specific nanozymes are determined based on their catalytic characteristics. To overcome the drawbacks of natural peroxidases, low cost nanozymes with good catalytic activity are needed. A comparison of catalytic performance and cost effectiveness was done. The relation between catalytic performance in terms of the turnover number (k_{cat}) per mass concentration and grams per dollar of a variety of nanozymes were compared. Nanozymes with different nanostructure were chosen for comparison.

33

Most nanozymes have high values of K_M for H_2O_2 corresponding to low affinity for hydrogen peroxide. The affinities of different nanozymes for hydrogen peroxide were plotted (**Figure 14).** Surprisingly, hafnium diboride nanozymes have the highest affinity for hydrogen peroxide than all the nanozymes we compared. This is an important result, especially for applications involving reactions with hydrogen peroxide.
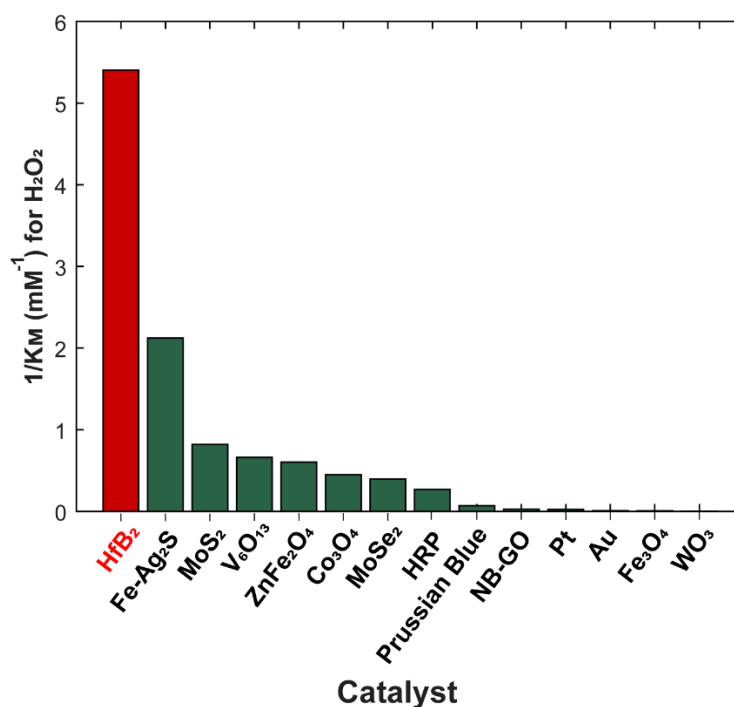

Figure 14: Affinity of catalysts for H_2O_2. The y-axis represents the reciprocal of the Michaelis constant for H_2O_2. [7,11,39,40,31–38]

One of the main drawbacks of natural enzymes is their high cost which is why lower cost nanozymes are needed. For instance, horseradish peroxidase has a price of around

$1500/gram which is higher than all the nanozymes used in this comparison. Most expensive nanozymes are the ones made of precious metals like Au and Pt with a minimum cost of \$300/gram. The most cost effective nanozymes include HfB_2, WO_3 graphene, Prussian blue and MoS_2 with prices lower than 5\$/gram. The catalytic performance and the cost were analyzed for different nanozymes in the literature (**Figure 15a and 15b**). The catalytic rate constants were calculated with the molar concentration of the chemical compound that make the nanozymes based on reported performance from the cited papers. The catalytic rate constant per mass concentration and the grams per dollar of nanozymes were then plotted in a logarithmic scale.

Platinum nanoparticles[37] showed the highest activity, but it has a cost of \$295/gram. HfB_2 nanozymes and Prussian Blue nanoparticles[36] showed optimal results in terms of the relation between activity and cost-effectiveness. Moreover, HfB_2 has a highest TMB turnover activity per cost between nanozymes with 2D-nanostructures. The turnover number of H_2O_2 substrate is lower than WO_3 when comparing 2D materials. This might be caused by the low concentration of H_2O_2 required to reach the maximal velocity. In **Figure 15c** the affinity of HfB_2/F77 with respect to TMB and the corresponding catalytic rate constant per mass were plotted. We can see that although the affinity is low compared to the rest of the nanozymes, the nanozyme could achieve high catalytic activity. The affinity of HfB_2/F77 with respect to H_2O_2 and the corresponding catalytic rate constant per mass for different nanozymes was also studied (**Figure 15d**). HfB_2/F77 withstands in the relation between affinity towards H_2O_2 and catalytic activity compared to other enzyme-mimics. These findings make HfB_2/F77 nanozyme a promising candidate for applications involving

35

extreme conditions since the nanozyme is capable to achieve high activity despite the high concentration of TMB required.
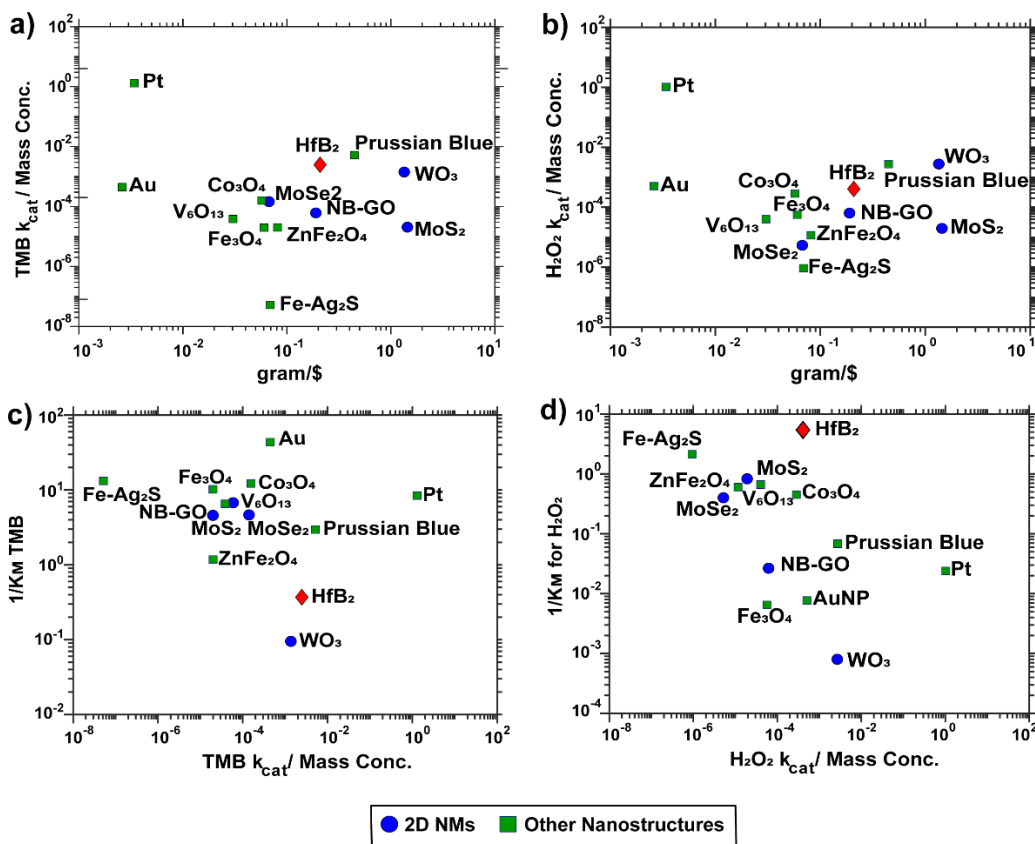
Figure 15: Catalytic performance and cost efficiency comparison between nanozymes. a) Relationship between catalytic constant per mass concentration for TMB and the grams of nanozyme per dollar. b) Relationship between catalytic constant per mass concentration for H_2O_2 and the grams of nanozyme per dollar. c) Relationship between TMB affinity and catalytic constant per mass concentration for TMB. d) Relationship between H_2O_2 affinity and catalytic constant per mass concentration for H_2O_2.[7,11,39,40,31–38]

Chapter 6

Conclusions and Future Work

It was demonstrated for the first time that hafnium diboride nanoflakes possess intrinsic peroxidase-like activity. Hence, a new nanozyme was added to the previously discovered peroxidase mimics. The nanoflakes were characterized by different material characterization techniques, and size and thickness distributions for the nanoflakes showed that the average exfoliated flake has a thickness of 13.9 nm and a size of 967 nm^2. The catalytic activity was characterized to find the ideal working condition in terms of pH, temperature and substrates concentrations. The determined optimal conditions to optimize the catalytic activity of HfB_2/F77 were pH4, 35℃, 7mM TMB and 6mM TMB. Catalytic parameters were determined by steady state kinetic experiments and the catalytic performance was compared with other nanozymes. Comparison showed that HfB_2/F77 has the highest affinity with respect to H_2O_2 and highest TMB turnover activity per cost between nanozymes with 2D-nanostructures. HfB_2 nanozymes along with Prussian Blue nanoparticles exhibit a foremost relation between activity and cost-effectiveness towards TMB turnover among the compared nanozymes.

The nanozyme dispersed by aqueous solution of F77 has the advantage of facile production through an environmentally friendly process of probe ultrasonication. Furthermore, the HfB_2/F77 nanozyme is cost-effective and it has a great catalytic performance. Finally, steady state kinetic assays revealed that the nanozyme has a very high affinity to hydrogen peroxide and the reaction mechanism follows a Ping-Pong mechanism.

The dispersing agent F77 enhances the biocompatibility of the nanozyme for future biological applications. The high affinity of the nanozyme for hydrogen peroxide opens the door for future possible applications. For instance, detecting biomolecules that are closely related to the generation of H_2O_2 by creating biosensors made of this nanozyme. Another possible future direction could be employing HfB_2/F77 for anti-bacterial applications due to the production of hydroxyl radicals from hydrogen peroxide.

REFERENCES

1. Binod, P., Papamichael, E., Varjani, S. & Sindhu, R. Introduction to Green Bioprocesses: Industrial Enzymes for Food Applications. in 1–8 (Springer, Singapore, 2019). doi:10.1007/978-981-13-3263-0_1

2. Shrivastava, A., Shrivastava, N. & Singh, P. K. Chapter 34 - Enzymes in Pharmaceutical Industry. in (ed. Kuddus, M. B. T.-E. in F. B.) 591–602 (Academic Press, 2019). doi:https://doi.org/10.1016/B978-0-12-813280-7.00034-7

3. An overview of immobilized enzyme technologies for dye and phenolic removal from wastewater. *J. Environ. Chem. Eng.* 7, 102961 (2019).

4. Liu, Y., Zheng, Y., Ding, D. & Guo, R. Switching Peroxidase-Mimic Activity of Protein Stabilized Platinum Nanozymes by Sulfide Ions: Substrate Dependence, Mechanism, and Detection. *Langmuir* 33, 13811–13820 (2017).

5. Lin, Y., Ren, J. & Qu, X. Nano-gold as artificial enzymes: Hidden talents. *Adv. Mater.* 26, 4200–4217 (2014).

6. Wang, X., Hu, Y. & Wei, H. Nanozymes in bionanotechnology: From sensing to therapeutics and beyond. *Inorg. Chem. Front.* 3, 41–60 (2016).

7. Gao, L. *et al.* Intrinsic peroxidase-like activity of ferromagnetic nanoparticles. *Nat. Nanotechnol.* 2, 577–583 (2007).

8. Huang, Y., Ren, J. & Qu, X. Nanozymes: Classification, Catalytic Mechanisms, Activity Regulation, and Applications. *Chem. Rev.* 119, 4357–4412 (2019).

9. Lfikar Temoçin, Z. *et al.* Immobilization of horseradish peroxidase on electrospun poly(vinyl alcohol)-polyacrylamide blend nanofiber membrane and its use in the conversion of phenol. *Polym. Bull.* 75, 1843–1865 (2018).

10. Zhang, Z. *et al.* Peroxidase-catalyzed chemiluminescence system and its application in immunoassay. *Talanta* 180, 260–270 (2018).

11. Kim, M. S. *et al.* N- and B-Codoped Graphene: A Strong Candidate to Replace Natural Peroxidase in Sensitive and Selective Bioassays. *ACS Nano* 13, 4312–4321 (2019).

12. Cai, S. *et al.* Pt74Ag26 nanoparticle-decorated ultrathin MoS2 nanosheets as novel peroxidase mimics for highly selective colorimetric detection of H2O2 and glucose. *Nanoscale* 8, 3685–3693 (2016).

13. Wang, Q. H., Kalantar-Zadeh, K., Kis, A., Coleman, J. N. & Strano, M. S. Electronics and optoelectronics of two-dimensional transition metal dichalcogenides. *Nat. Nanotechnol.* 7, 699–712 (2012).

14. Puthirath Balan, A. *et al.* Exfoliation of a non-van der Waals material from iron ore hematite. *Nat. Nanotechnol.* 13, 602–609 (2018).

15. Backes, C. *et al.* Guidelines for exfoliation, characterization and processing of layered materials produced by liquid exfoliation. *Chem. Mater.* 29, 243–255 (2017).

16. Pitto-Barry, A. & Barry, N. P. E. Pluronic® block-copolymers in medicine: From chemical and biological versatility to rationalisation and clinical advances. *Polym. Chem.* 5, 3291–3297 (2014).

17. Seo, J.-W. T., Green, A. A., Antaris, A. L. & Hersam, M. C. High-Concentration Aqueous Dispersions of Graphene Using Nonionic, Biocompatible Block Copolymers. *J. Phys. Chem. Lett* 2, 1004–1008 (2011).

18. Sani, E. *et al.* Process and composition dependence of optical properties of zirconium, hafnium and tantalum borides for solar receiver applications. *Sol. Energy Mater. Sol. Cells* 155, 368–377 (2016).

19. Wagner, F. R., Baranov, A. I., Grin, Y. & Kohout, M. A position-space view on chemical bonding in metal diborides with AlB 2 type of crystal structure. *Zeitschrift fur Anorg. und Allg. Chemie* 639, 2025–2035 (2013).

20. Chatakondu, K., Green, M. L. H., Thompson, M. E. & Suslick, K. S. The enhancement of intercalation reactions by ultrasound. *J. Chem. Soc. Chem. Commun.* 900–901 (1987). doi:10.1039/C39870000900

21. Gupta, A., Arunachalam, V. & Vasudevan, S. Water dispersible, positively and negatively charged MoS2 nanosheets: Surface chemistry and the role of surfactant binding. *J. Phys. Chem. Lett.* 6, 739–744 (2015).

22. Notley, S. M. Highly concentrated aqueous suspensions of graphene through ultrasonic exfoliation with continuous surfactant addition. *Langmuir* 28, 14110–14113 (2012).

23. Marquez, L. A. & Dunford, H. B. Mechanism of the oxidation of 3,5,3',5'-tetramethylbenzidine by myeloperoxidase determined by transient- and steady-state kinetics. *Biochemistry* 36, 9349–9355 (1997).

24. Gao, L. *et al.* Intrinsic peroxidase-like activity of ferromagnetic nanoparticles. 577–583 (2007). doi:10.1038/nnano.2007.260

25. Xia, X. *et al.* Pd-Ir Core-Shell Nanocubes: A Type of Highly Efficient and Versatile Peroxidase Mimic. *ACS Nano* 9, 9994–10004 (2015).

26. Chen, Y., Chen, T., Wu, X. & Yang, G. CuMnO 2 nanoflakes as pH-switchable catalysts with multiple enzyme-like activities for cysteine detection. *Sensors Actuators, B Chem.* 279, 374–384 (2019).

27. Cho, Y. S. & Lim, H. S. Comparison of various estimation methods for the parameters of Michaelis–Menten equation based on in vitro elimination kinetic simulation data. *Transl. Clin. Pharmacol.* 26, 39–47 (2018).

28. Porter, D. J. & Bright, H. J. The mechanism of oxidation of nitroalkanes by horseradish peroxidase. *J. Biol. Chem.* 258, 9913–9924 (1983).

29. Song, Y., Qu, K., Zhao, C., Ren, J. & Qu, X. Graphene oxide: Intrinsic peroxidase catalytic activity and its application to glucose detection. *Adv. Mater.* 22, 2206–2210 (2010).

30. Yin, W. *et al.* Functionalized Nano-MoS2 with Peroxidase Catalytic and Near-Infrared Photothermal Activities for Safe and Synergetic Wound Antibacterial Applications. *ACS Nano* 10, 11000–11011 (2016).

31. Li, Z. *et al.* Colorimetric determination of xanthine in urine based on peroxidase-like activity of WO3 nanosheets. *Talanta* 204, 278–284 (2019).

32. Ding, Y. *et al.* Fe-doped Ag 2 S with excellent peroxidase-like activity for colorimetric determination of H 2 O 2. *J. Alloys Compd.* 785, 1189–1197 (2019).

33. Li, H. *et al.* Intrinsic Triple-Enzyme Mimetic Activity of V 6 O 13 Nanotextiles: Mechanism Investigation and Colorimetric and Fluorescent Detections. *Ind. Eng. Chem. Res.* 57, 2416–2425 (2018).

34. Huang, X. W. *et al.* Silk fibroin-assisted exfoliation and functionalization of transition metal dichalcogenide nanosheets for antibacterial wound dressings. *Nanoscale* 9, 17193–17198 (2017).

35. Liu, Y., Xiang, Y., Ding, D. & Guo, R. Structural effects of amphiphilic protein/gold nanoparticle hybrid based nanozyme on peroxidase-like activity and silver-mediated inhibition. *RSC Adv.* 6, 112435–112444 (2016).

36. Zhang, W. *et al.* Prussian Blue Nanoparticles as Multienzyme Mimetics and Reactive Oxygen Species Scavengers. *J. Am. Chem. Soc.* 138, 5860–5865 (2016).

37. Li, W. *et al.* BSA-stabilized Pt nanozyme for peroxidase mimetics and its application on colorimetric detection of mercury(II) ions. *Biosens. Bioelectron.* 66, 251–258 (2015).

38. Mu, J., Wang, Y., Zhao, M. & Zhang, L. Intrinsic peroxidase-like activity and catalase-like activity of Co3O4 nanoparticles. *Chem. Commun.* 48, 2540–2542 (2012).

39.   Su, L. *et al.* Colorimetric detection of urine glucose based ZnFe2O4 magnetic nanoparticles. *Anal. Chem.* 84, 5753–5758 (2012).

40.   Yu, J. *et al.* Peroxidase-like activity of MoS2 nanoflakes with different modifications and their application for H2O2 and glucose detection. *J. Mater. Chem. B* 6, 487–498 (2018).